CRACKING ANALYSIS OF REINFORCED CONCRETE BEAMS USING A FINITE – DISCRETE ELEMENT METHODS APPROACH

CECILE OLIVER-LEBLOND[*], BENJAMIN RICHARD[†], ARNAUD DELAPLACE[**] AND FREDERIC RAGUENEAU[*]

[*] LMT-Cachan
ENS Cachan/CNRS/Université Paris 6/UniverSud Paris
61 avenue du Président Wilson, 94230 Cachan, France
e-mail: oliver@lmt.ens-cachan.fr, ragueneau@lmt.ens-cachan.fr

[†] CEA-Saclay
CEA/DEN/DANS/DM2S/SEMT/Laboratoire d'Etudes de Mécanique Sismique,
91191 Gif-sur-Yvette Cedex - France
e-mail: Benjamin.RICHARD@cea.fr

[**] Lafarge Centre de Recherche
95 rue de Montmurier, 38291 Saint Quentin Fallavier, France
e-mail: arnaud.delaplace@pole-technologique.lafarge.com

Key words: Cohesive fracture, Damage mechanics, cracking, finite element analysis

Abstract: Combining the use of finite element analysis and a discrete element approach, this contribution aims at proposing a new post-treatment technique to help one in computing the cracking openings in complex reinforced concrete structures subject to mechanical loadings.

1 INTRODUCTION

Concerning civil engineering structures issue, the prediction of cracking remains a main concern regarding the behaviour of concrete elements, or reinforced concrete elements. The effects of a crack on the durability of a structure are a major concern as long as the predictivity improvement for the numerical analysis is required. Not only the crack pattern but also the crack features such as spacing, openings, rugosity and tortuosity have to be addressed at a structural scale.

The purpose of the present study is therefore to propose an original technique [1] allowing the use of finite element models [3] at a structural scale and a decoupled local analysis of some interesting zones for which a discrete element model is relevant [2]. Two distinct numerical analyses are performed emphasising their respective efficiency. First, a three dimensional non linear finite element analysis using damage mechanics based constitutive equations is introduced. From the damage pattern and the nodal displacement field, a second analysis is performed in order to evaluate discrete crack opening values, considering some critical zones. The discrete element method is here employed as a post-processing operator allowing focusing the analysis on some critical parts of the whole structure which has been entirely evaluated at a coarse and large scale. Each family of models is employed in its better application field: macroscopic nonlinear description of the structure concerning the continuous method

and mesoscopic analysis of a crack for the discrete model. Any characteristic length is no longer introduced in the region of interest for cracking analysis.

In a first part of the contribution, the theoretical and numerical frameworks of the developments are presented. The second part of the paper is devoted to a numerical case-study. The relevancy of the use of such a non-intrusive and decoupled method for a two scale analysis is appreciated within a non linear analysis of a reinforced concrete beam subject to bending moments (CEOS.fr project). The relevancy of this approach for combining finite element and discrete modelling is emphasised through comparisons with experimental results.

2 NUMERICAL TOOLS

The method developed here is inspired by the sub-modeling techniques often used for industrial problems because of their simplicity. Those methods consist in a global analysis of the structure and a local analysis of the Region Of Interest (ROI). The boundary conditions applied on the local model are displacements which are interpolated from the global solution. The method is non-intrusive because it only uses available input and output (nodal displacements).

2.1 General method

The sub-modeling technique is composed of the following steps:

- Global analysis of the whole structure with a non-linear finite element model including damage;
- Identification and cutting of the ROI, which is the region of damage concentration;
- Extraction and interpolation of the displacements from the global mesh to the local mesh;
- Local analysis of the ROI with a discrete element model.

No global correction from the local model to the global one, through forces for example,

is performed. Indeed, the local analysis is considered as a post-processing tool which only gives valuable data on the kinematic and features of the crack. That local description does not give any more information on the global mechanical behavior than what the global model has already given. Indeed, the two models complete each other by describing in their own different way the same phenomenon, namely the crack. The global behavior of the crack, its effect on the stress field, is taken into account through the damage variable of the non-linear finite element model. The reanalysis with the discrete element model generates not only a refinement around the crack but also a fine representation of the local behavior of the crack.

The boundary conditions of the local computation are obtained from the global computation all along the non-free surfaces ∂R_u of the ROI. Those boundary conditions are Dirichlet boundary conditions, which is common for sub-modeling techniques. The natural way to transfer the displacement field from the global to the local mesh is to use the shape functions (N_j) of the finite elements used at the global scale. Then, the displacement $U^D(x_k^D)$ at each nuclei x_k^D of the cells related to the discrete element model along the ROI boundary are directly obtained by:

$$U^D(x_k^D) = \sum_j N_j(x_k^D)U_j^h \qquad (1)$$

The advantage of this strategy, where the computation is performed twice on the region of interest (first with the global model and then with the local model), is that an estimator of the gap between both models is not limited to the ROI boundaries but can be extended over the whole region. Then, one can distinguish the different areas where the models are more or less in agreement with each other. It must be noted that by imposing the global displacements on the local boundaries, the two models are always in agreement on those regions and the comparison is in fact only

relevant on the rest of the region. We propose a gap estimator based on the displacement fields obtained with the two models. As the displacement field at the local scale is only computed at the cells' nuclei, we compute the gap estimator field at the cells' nuclei, using the shape functions of the finite elements in order to compute the global scale displacement. The gap at the point x_k^D is:

$$e(x_k^D) = \frac{\left\| U^D(x_k^D) - \sum_j N_j(x_k^D) U_j^h \right\|_2}{\left\| U^D(x_k^D) \right\|_2} \qquad (2)$$

2.3 Finite element constitutive equations

Concerning the model at the macroscopic and continuous finite element scale, a three dimensional set of constitutive equations for modelling quasi-brittle materials such as concrete is presented. It is formulated within the framework of irreversible processes thermodynamics in order to fulfil physical consistency [4]. A single scalar damage variable has been introduced in order to take into account nonlinearities due to micro-cracking. The sliding influence and the partial stiffness recovery have been considered for cyclic loadings.

To separate the difficulties, the cracked behaviour will be assumed to be separable into two independent behaviours [3]. For the hydrostatic strain mechanisms, only cracks opening and closing are considered. The frictional sliding is only treated on the deviatoric part of the strain and stress tensors. Figure 1 gives a schematic representation of such a hypothesis. These considerations lead to a decomposition of the strain energy into two different parts respectively due to the spherical and the deviatoric components. This feature is one of the key points for taking into account damage and sliding properly as discussed below.

$$\rho\Psi = \frac{1}{2}\left\{ \frac{\kappa}{3}\left((1-d) < \varepsilon_{kk} >_+^2 - < -\varepsilon_{kk} >_+^2 \right) + 2(1-d)\mu\varepsilon_{ij}^D \varepsilon_{ij}^D \right.$$
$$\left. + 2d\mu\left(\varepsilon_{ij}^D - \varepsilon_{ij}^\pi\right)\left(\varepsilon_{ij}^D - \varepsilon_{ij}^\pi\right) + \gamma\alpha_{ij}\alpha_{ij} \right\} + H(z) \qquad (3)$$

where ρ is the material density, κ and μ are the bulk and shear coefficients respectively. ε_{ij} is the second order total strain tensor, δ_{ij} is the second order Kronecker's tensor, $\varepsilon_{ij}^D = \varepsilon_{ij} - \frac{1}{3}\varepsilon_{kk}\delta_{ij}$ is the second order deviatoric total strain tensor and d is the scalar damage variable (0 for virgin material and 1 for failed material). ε_{ij}^π is the second order sliding tensor. It can be noted that the sliding tensor needs to be purely deviatoric in order to preserve the consistency of the formulation. γ is a material parameter, α_{ij} is the second order tensor associated to the kinematics hardening, z is the internal variable corresponding to the isotropic hardening and H its consolidation function.

The state laws are obtained by simple derivation of the thermodynamic potential regarding the state variables (strain, sliding strains and damage). For example concerning the Cauchy stress tensor:

$$\sigma_{ij} = \frac{\partial \rho\Psi}{\partial \varepsilon_{ij}} \qquad (4)$$

The evolution of the internal variables are subject to complementary equations based on the respect of threshold functions. For damage, based on an energy type criterion, one can define the following criterion:

$$f_d = \bar{Y} - (Y_0 + Z) \qquad (5)$$

where $\bar{Y}$ denotes energy-type variable driving damage and Y_0, an initial threshold.

In order to manage sliding and kinematic hardening, a surface without any threshold is introduced in order to manage sliding mechanism associated to kinematics hardening. It takes the form of a Von Mises criterion (without hydrostatic effects)

expressed as:

$$f_\pi = \sqrt{\frac{3}{2}(s_{ij} - X_{ij})(s_{ij} - X_{ij})} \qquad (6)$$

where s_{ij} is the deviatoric part of the Cauchy's stress tensor. Differently from the previous case, the flow rules are supposed not to be associated ones. From the maximum dissipation principle, the plastic potential can be defined as [5]:

$$\varphi_\pi = \sqrt{\frac{3}{2}(s_{ij} - X_{ij})(s_{ij} - X_{ij})} + \frac{a}{2}X_{ij}X_{ij} \qquad (7)$$

The cyclic response of this model for a compressive state of stresses is presented in figure 1.
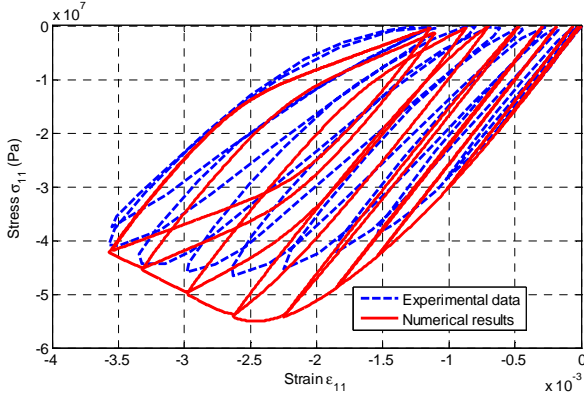
Figure 1: Comparison between numerical and experimental results related to a local cyclic compression stress state.

More details concerning the model, its numerical implementation as well as its identification can de found in [3].

2.3 Discrete element model

A particle-based discrete model is used in order to compute a fine description of the crack. With this approach, the material is described as a particle assembly. A crack is naturally obtained if a bond linking two particles breaks. A Voronoi tessellation is used, allowing an efficient and easy mesh generation. The particle nuclei are randomly generated on a grid [2] in order to control the boundary conditions. Cohesion forces can be equally represented either by springs at the

interface of neighboring particles or by beams linking the nuclei of the particles (lattice model). Euler-Bernoulli beams are chosen in the model used in this study. Then, four parameters have to be identified: the length ℓ_b, the cross section area A_b, the inertia I_b (or the adimensional parameter $\alpha = I_b/I_0$ where I_0 is the inertia of the equivalent circular section) and the elastic modulus E_b of the beam. The first two parameters are prescribed by the mesh geometry and are different for each beam. The last two parameters are supposed equal for all beams and are identified in order to obtain the elastic properties of the material, E and ν, respectively Young's modulus and Poisson's ratio. Note that if necessary, one can compute contact forces between unlinked particles, for example for cyclic loading with crack opening and closing.

The non-linear behavior of the material is obtained by considering that the beam obey a brittle behavior. The displacements of the particle nuclei are the primary measure in this model. Hence, a displacement-based breaking threshold P_{ij} is used here. Only two mechanisms contribute to the breaking of the beam: elongation and flexion. Thus, the breaking threshold depends on the beam strain and on the rotations of the particles (respectively i and j) linked by the beam. It is written as:

$$P_{ij} = \left(\frac{\varepsilon_{ij}}{\varepsilon_{ij}^{cr}}\right)^2 + \frac{|\theta_i - \theta_j|}{\theta_{ij}^{cr}} > 1 \qquad (8)$$

The critical strain ε_{ij}^{cr} and the critical rotation θ_{ij}^{cr} of the beam $i - j$ are assigned to the beam $i - j$ using a random number generator according to the Weibull distribution, as proposed by [6].

2.4 Model calibration

The global model requires eight material parameters: two related to the elasticity mechanism, three related to the isotropic damage mechanism, two related to the internal sliding and one related to the non-local mechanism. In order to provide the best set of

parameters, they are all identified with respect to the available experimental information from tensile tests, compressive tests and three- point bending tests. Structural tests are used to allow for the calibration of the internal length (due to the nonlocal damage theory used).

The local model has two parameters related to elasticity and four parameters related to fracture. A tensile test on a dog-bone shaped specimen is performed first with the global model and then with the local model. Hence, the parameters of the local model are calibrated by fitting the local response—namely the complete load-displacement curve and the dissipated energy-displacement curve—and the global response. The complete load-displacement curves and dissipated energy-displacement curves obtained with the global and the local models on the dog-bone shaped specimen are reported in figure 2 and 3. A good agreement between the two models is obtained with the local modelling.
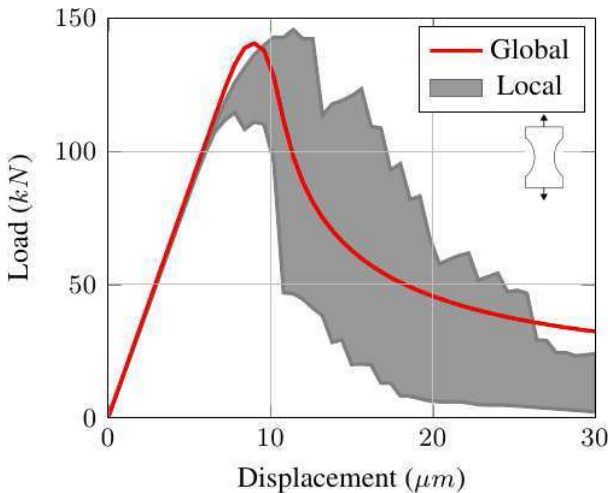
Figure 2: Comparison between Finite Element and Discrete Element model for a dog-bone specimen (load-displacement comparisons)

This calibration corresponds to a classical concrete material showing a Young's modulus E = 34 GPa, a Poisson's ratio of 0.2, a tensile strength of 3.5 MPa and a compressive peak load of 53 MPa.
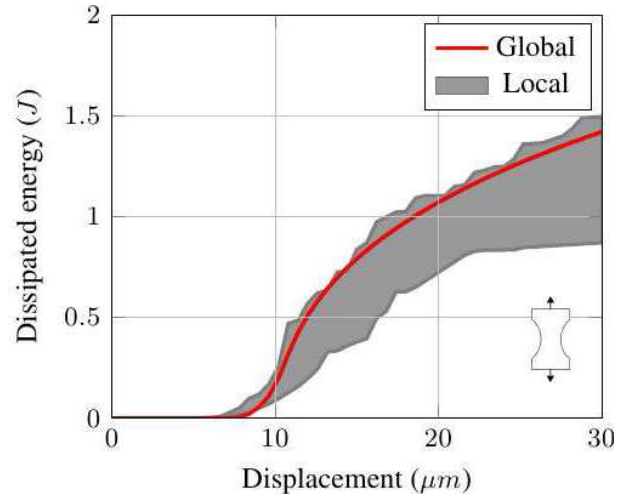

Figure 3: Comparison between Finite Element and Discrete Element model for a dog-bone specimen (dissipated energy comparisons).

3 REINFORCED CONCRETE CASE-STUDY

3.1 Experimental set-up description

To illustrate the possibilities offered by the approach to handle 3D problems, a reinforced concrete beam has been considered. The beam has been experimentally investigated within the framework of the project CEOS.fr supported by the French national agency for research. The specimen is 1600 mm large, 800 high and 6100 long. It has been reinforced by 8 steel bars (8HA16) in the top part (compression part) and by 16 steel bars (16HA32) in the bottom part (tension part). 19 stirrups (HA16) have also been considered with spacing equal to 350 mm far from the supports and equal to 200 close to them.
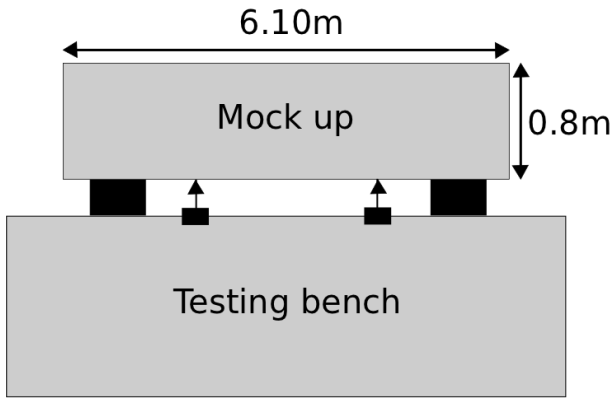
Figure 4: General experimental set-up

Figure 5: ¼ of the beam using 8 node meshing

The reinforced concrete specimen has been clamped to a reaction reinforced concrete block through rigid bars. Two lines of jacks have been put between the specimen and the support in order to create a four point bending loading. A sketch of the loading conditions can be observed in figure 4. The loading is controlled by prescribing the loads through the jacks.

3.2 Finite element analysis

As the geometric dimensions of the specimens are rather high, 3D effects may play a preponderant role regarding the mechanical behavior. The choice to consider a 3D finite element model has therefore been made. For symmetry reasons, only a quarter of the beam has been modeled. The longitudinal reinforcing steel bars have been modeled by 8-node finite elements although the stirrups have been considered as bar elements. The concrete is meshed by 8-node finite elements. Some pictures of the finite element mesh can be observed in figure 5. The reinforced concrete beam has been assumed as being simply supported (figure 6). Additional boundary conditions related to the symmetry have also been taken into account. The concrete is modeled by the constitutive law that has been exposed in section 2 and the steel reinforcing bars are assumed to follow an elastic-plastic constitutive law.
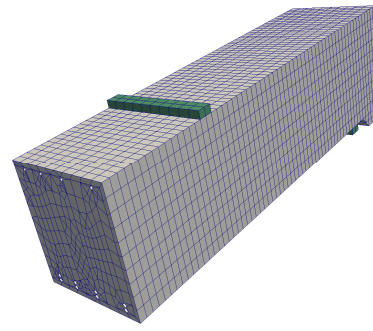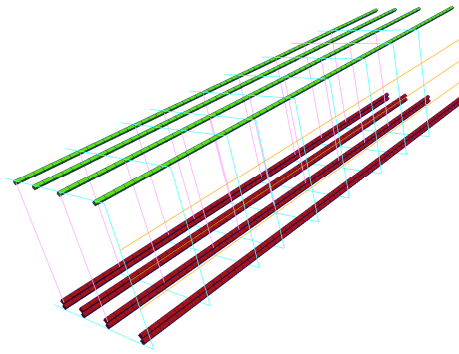

Figure 6: 3D meshing of the steel rebar

The global response is compared to the experimental results in the following figure. Three levels of loading have been analysed in terms of damage field and cracking (figures 8, 9 and 10).
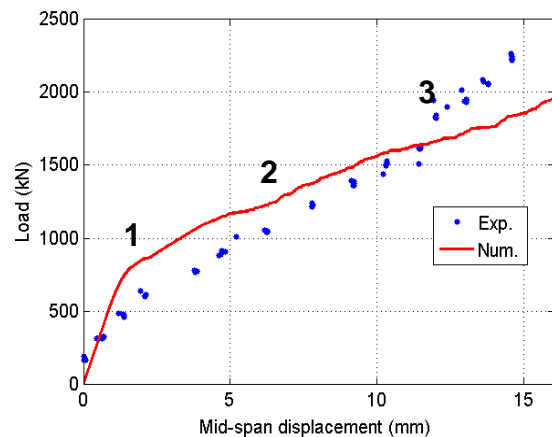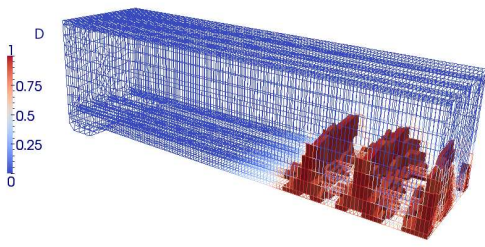

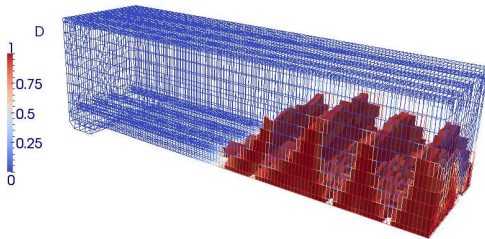**Figure 7: Load-displacements comparisons**

6

Figure 8: Damage map for the level 1

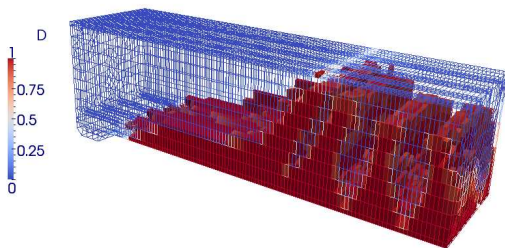**Figure 9: Damage map for the level 2**

Figure 10: Damage map for the level 3

3.2 Discrete element local re-analysis

A first attempt has been maid to evaluate the possibility of using such an approach to observe the discrete cracking in such structures. The three main cracks have been re-analysed using the previous methodology as shown in figure 11.

In figure 12, the cracks are superimposed with the damage map emphasizing the good agreement between a discrete quantity and the continuous one obtained using standard numerical tools dedicated to nonlinear structural analysis. In the same way, the relevancy of the approach is shown by plotting

the cracks on the longitudinal displacement field obtained thanks to the global and continuous finite element analysis.
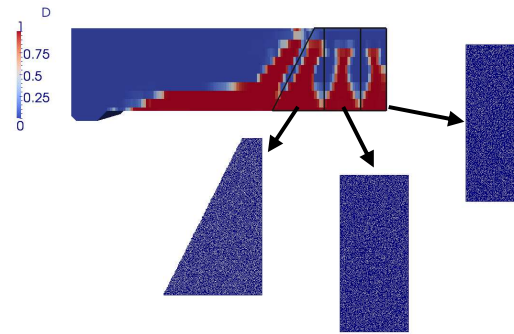

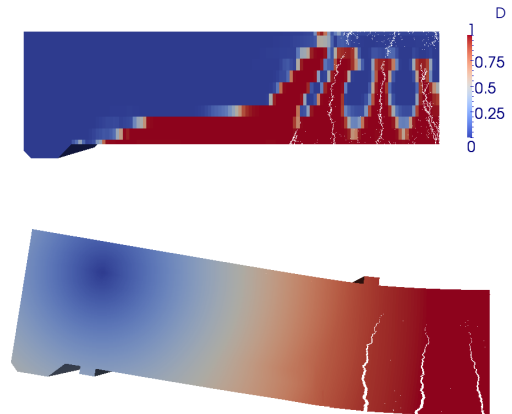**Figure 11: ROI definition regarding the 3 main damage areas**

Figure 12: Cracks regarding continuous displacement field and damage pattern.

4 CONCLUSIONS

A general procedure aiming at analyzing finite element results in terms of discrete quantities such as cracks has been presented. The continuous and macroscopic nonlinear set of constitutive equations based on damage mechanics as well as the discrete element approach used at the local level have been also addressed. The link between the two levels of modeling is ensured thanks to kinematic constraints. A parameters identification procedure based on the level of dissipated

energy between the two approaches has been established. First results obtained on concrete structures and reinforced concrete structures confirm the capability of such a framework to handle discontinuous cracks within continuous media.

In the near future, more efforts should be paid in quantitative comparisons with experimental data regarding crack openings for the discrete model and strains for the continuous one. For cracking in reinforced concrete structure, the 3D behaviour of the concrete near the reinforcement bars is of major importance. We expect that such a 3D local reanalysis will help one to better understand the crack propagation kinematic under monotonic loading but also when sustaining cyclic loading.

REFERENCES

[1] Oliver-Leblond C., Delaplace A., Ragueneau F. and Richard B. Non-intrusive global/local analysis for the study of fine cracking, Int. J. Numer. Anal. Meth. Geomech, to *be published*.

[2] Delaplace A., Desmorat R. Discrete 3d model as complimentary numerical testing for anisotropic damage, Int J. Fract 2007.

[3] Richard B., Ragueneau F., Crémona C. & Adelaide L., Isotropic continuum damage mechanics for concrete under cyclic loading: stiffness recovery, inelastic strains and *frictional sliding*, *Engineering Fracture Mechanics* , Engineering Fracture Mechanics**, 77(8)**, pp. 1203-1223, 2010.

[4] Lemaître J, Chaboche JL. Solid material mecahnics, Dunod, 2004.

[5] Armstrong PJ, Frederick CO. A mathematical representation of the multiaxial Bauschinger effect, G.E.G.B., Report RD/B/N. 1966;731

[6] Van Mier JGM, Van Vliet MRA,Wang TK. Fracture mechanisms in particle composites: statistical aspects in lattice type analysis. Mech. Mater 2002; 34:705–724.